A Study on the Evaluation of Exposure Dose and Image Quality as a Function of Exposure Conditions in Head Radiography for Children

Sung-Hyun Choi[1], Chang-Gi Kong[2] and Yong-Soon Park[3,*]

[1]*Department of Radiology, Kyung Hee University Hospital at Gang-dong, 892, Dongnam-ro, Gangdong-gu, Seoul 05278, Republic of Korea*
[2]*Department of Radiology, Cheom Dan Hospital, 59, Cheomdanjungang-ro 170beon-gil, Gwangsan-gu, Gwangju 62274, Republic of Korea*
[3]*Department of Radiological Technology, Gwangju Health University, 73, Bungmun-daero 419 beon-gil, Gwangsan-gu, Gwangju 62271, Republic of Korea*

Abstract - In this study, we analyzed exposure dose and image quality as a function of exposure conditions in head radiography in radiation-sensitive children less than five years old. To compare exposure doses, we used measures of the absorbed dose, such as DAP and ESD. For image quality, the PSNR was used to quantitatively assess noise characteristics. The SRS-78 program was used to simulate changes in X-ray beam quality in order to determine optimal exposure conditions. The DICOM header information of Infinitt Piview was used to examine skull AP and lateral radiography conditions for head radiographies performed in children less than five years old between January 2018 and December 2019. Average exposure conditions and EI and DAP values were calculated. An acryl phantom was used as a simulated patient, and a VICTOREEN NERO mAx 8000 and ionization chamber were used to calculate the ESD value and entrance surface dose as a function of kVp and mAs. Sample images for various exposure conditions were obtained to measure and analyze SNR, PSNR, RMSE, and MAE. Then, simulations were conducted to study the characteristics of photon energy and spectrum changes relating to changes in kV. For the first head radiograph, the ESD value was 0.611 mGy using average exposure conditions of 66 kVp and 12.5 mAs. As kVp and mAs were increased, the DAP and ESD values also increased, while the EI value decreased. When kVp and mAs were decreased, the DAP and ESD values also deceased, while the EI value increased. For the second radiograph, in which there was no degradation of image quality, the ESD value was 1.596 mGy at 32 mAs and 0.308 mGy at 6.3 mAs (for a fixed kVp), a 5.2-fold difference from the first radiograph. When the value of mAs was fixed, the ESD value was 1.029 mGy at 81 kVp and 0.314 mGy at 52 kVp, a 3.3-fold difference from the first radiograph. The average photon energy was 43.6 keV at 81 kV, 38.1 keV at 66 kV, and 33 keV at 52 kV. The air kerma value was 169.8 at 81 kV, 119.8 at 66 kV, and 75.27 at 52 kV, a 2.25-fold difference. The first HVL was 2.868 mmAl at 81 kV, 2.311 mmAl at 66 kV, and 1.832 mmAl at 52 kV, a difference in beam quality of about 1.56-fold. This study confirmed that the exposure dose reached a maximum difference of 5.2-fold without the degradation of image quality and with changes in kVp and mAs. The first step toward reductions in exposure doses is to educate hospitals that radiation exposure among children is a problem. We also hypothesize that interest in and study of radiation exposure among children will lead to the acquisition of good-quality images with reductions in radiation dose.

Key words : Children, EI, DAP, ESD, PSNR

* Corresponding author: Yong-Soon Park, Tel. +82-62-958-7771, Fax. +82-62-958-7669, E-mail. peter@ghu.ac.kr

INTRODUCTION

X-rays have become an indispensable in modern medicine to visualize the human body through film or a detector in order to make diagnoses. Recent developments have begun a transition from film/screen technologies such as X-rays to digital radiation technologies such as computed radiography (CR) and digital radiography (DR). However, the development of such equipment has enabled very easy image acquisition, which has led to an increase in the number of cases in which radiation is used for examination (sometimes more than once) as well as an increase in radiation exposure (Jung 2011).

The use of radiation for patient examination must be justified by the diagnostic value of the images obtained. To optimize radiation protection for the patient, images should obtained in accordance with the 'as low as reasonably achievable (ALARA)' principle, in which the radiation dose is minimized (ICRP 1990). In practice, radiation doses vary according to the examination site, medical institution and country. A report by the United Nations Scientific Committee on the Effects of Atomic Radiation (UNSCEAR) in 2000 demonstrated that even though the same radiology examinations are performed in many countries of the European Community (EC) and the Organization for Economic Cooperation and Development (OECD), patient doses differed by factors of 10-100, depending on the medical institution (UNSCEAR 2000).

According to a study conducted in a children's hospital in the US, 43% of general X-ray radiographies for children resulted in excessive exposure, with exposure doses on average four times higher than necessary. In film/screen methods, excessive exposure leads to blackening phenomena. In DR, on the other hand, images are corrected via a digital process to ensure that excessive exposure does not lead to such blackening phenomena, and thereby improving the signal-to-noise ratio (SNR) (Don 2004). Unfortunately, excessive exposure does not seem realistic to either the examiner or the patient, even though it increases the probability of cancer development. According to one study, general X-ray radiography may increase the risk of pediatric leukemia and breast cancer (Shu *et al*. 2002), and increases the occurrence of hepatoblastomas in underweight premature babies (Tanimura *et al*. 1998).

Unlike adults, children have a wide variety of body shapes as they grow from newborns to adolescents. Moreover, children have a 10∼20 times higher sensitivity to radiation than adults, and thus it is much more important to manage exposure doses for children. The frequency of radiography use is lower in children than in adults, but due to economic and cultural advances, development of industry and transportation, and complexity and diversification of living environments, the risk of accidents among children has increased. Consequently, more and more children visit emergency rooms and hospitals (Yun *et al*. 2009), which have resulted in an increasing number of pediatric patients who undergo diagnostic radiography. Radiography is also sometimes performed in neonatal intensive care units several times in a day if it is deemed to be necessary. Therefore, in order to reduce exposure in children, an examination of proper exposure conditions that takes children's body shape into account is necessary. Such a study should analyze how to restrict the radiation exposure site, refrain from unnecessary and repeated radiographs, and shield organs that are sensitive to radiation.

In this study, exposure dose and image quality were compared under various exposure conditions for head radiographs of children less than five years old. The exposure dose was compared using the dose area product (DAP) and NERO MAX 8000. To quantitatively evaluate image quality, the PSNR was used. The SRS-78 program was used to simulate changes in X-ray beam quality in order to suggest proper exposure conditions.

MEASUREMENT EQUIPMENT AND METHOD

1. Experimental Equipment

The X-ray generator used in this study was a Philips Diagnost VR (IR-1100-150) that was digital radiography equipment and based on amorphous silicon (a-Si) in indirect radiography (Fig. 1).

In order to obtain precise measurement values, quality control (QC) was performed for all of the images in the final experiment. The results were as follows.

The percent average error (PAE) of the tube voltage was 0.56% (less than ± 10%), which as suitable for the set value. When reproducibility of the exposure dose was evaluated, the coefficient of variation (CV) was measured at 0.00133 (0.05 or less). With regard to the size of the X-ray tube focus, the shapes of the FLUKE MODEL 07-591 Focal Spot

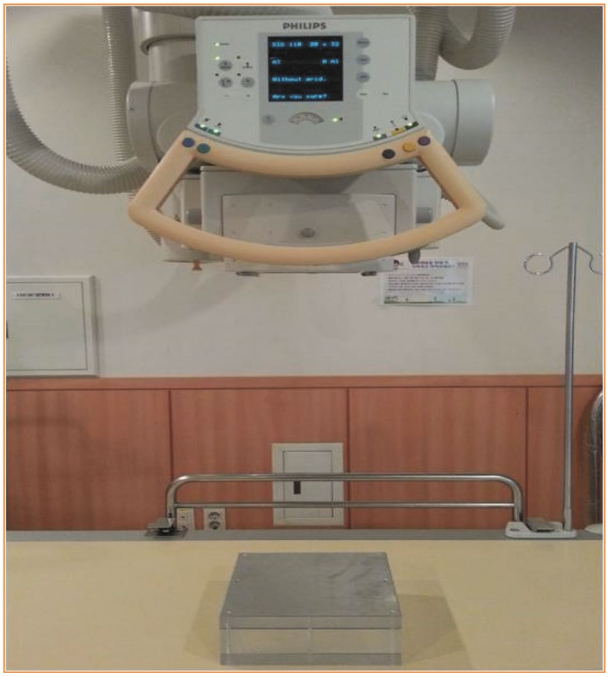

Fig. 1. Philips Digital Diagnost VR.

Test Tool Bars were found to be in 13 groups for all of large focus and small focus, which was suitable. In the half value layer (HVL) test, the HVL was measured at 3.76 mmAl (higher than the minimum HVL of 2.3 mmAl), which was suitable.

Based on the image quality control tests the objectivity and validity of the experiment results were confirmed within error under all the conditions.

2. Experimental Methods

2.1 Dose Evaluation

To investigate average exposure conditions used on children in clinical practice, this study targeted children who visited our hospital from January 2018 to December 2019. DICOM header information of Infinitt Piview (version 5.0.9.52) was used to examine the skull anterior posterior (AP) and skull lateral radiography conditions of children less than five years old before the average exposure conditions and exposure index (EI) and DAP were calculated (Table 1 and Fig. 2).

Acryl material was used to manufacture FRUKE Model 76-2 Series Phantoms in accordance with examination conditions before the simulated patient was used to replace the children (Fig. 3).

The first experimental conditions fixed kVp and adjusted

Table 1. The tofu inspection of average exposure conditions, and EI and DAP values of radiographs of children less than 5 years old

Legion		kVp	mAs	EI[a]	DAP[b] (Gy·cm^2)
SKULL	AP[c]	65.46	12.8	289.83	3.351
	Lateral	65.51	11.09	236.1	3.1

[a]EI is exposure index, [b]DAP is dose area product, [c]AP is anterior posterior.

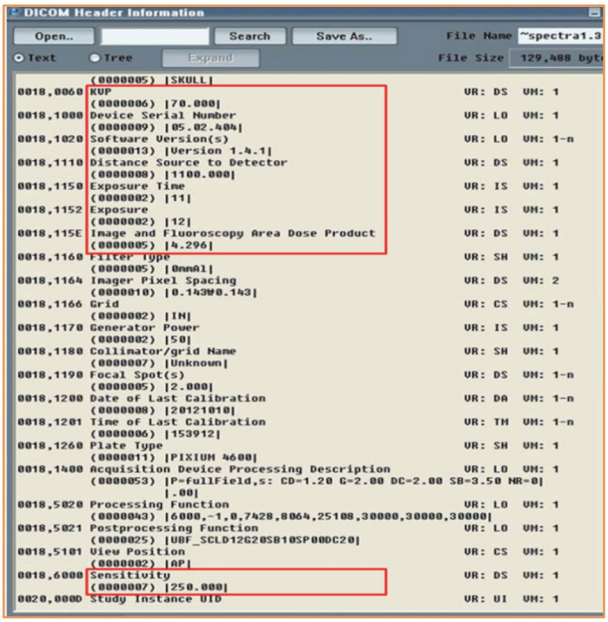

Fig. 2. DICOM Header Information.

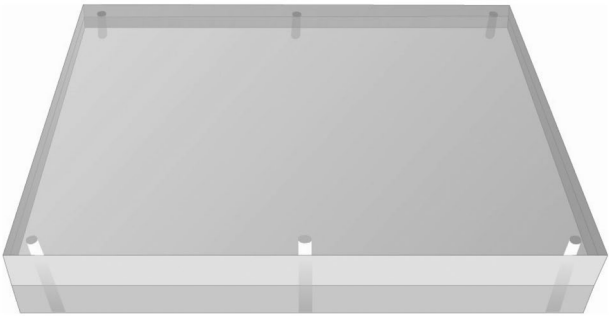

Fig. 3. FRUKE Model 76-2 Series Phantom.

mAs in 16 stages. The second experiment fixed the mAs and adjusted kVp in 16 stages. EI and DAP values were calculated for all experimental conditions based on the DICOM header information from the experimental image. A VICTOREEN NERO mAx 8000 and ionization chamber were used to measure the exposure dose before the entrance

(a) (b) (c)

Fig. 4. (a) NERO mAx 8000, (b) Ion Chamber, and (c) Filter card (W/A1).

surface dose (ESD) was calculated (Fig. 4).

The DAP can be measured by using a large-area ionization chamber located in the outlet of the X-ray tube. For new-model DR systems, the DAP can be calculated by using generator data and location information. If a proper monitoring device is installed in the X-ray equipment, the area dose can be calculated without interfering with image acquisition (Eq. 1) (ICRP 2003).

$$\mathrm{DAP}(\mathrm{Gy}\cdot\mathrm{cm}^2) = \mathrm{Dose} \times \mathrm{Area} \quad (1)$$

The exposure dose can be measured by the ionization chamber dosimeter, which is used to measure X-rays and γ-rays. In general radiography, the exposure dose of a patient, which is a physical quantity with clear standards, is measured in the method that uses exposure dose that can secure traceability to evaluate absorbed dose on skin surface where human body is exposed to X-ray. For this reason, the dosimeter used in study is an ionization chamber dosimeter where air is used as the ionization gas. Calibration is important because it is the determination of the relationship between a measured indication value and its reference quantity, based on the response of the dosimeter. When the ratio of the indication value obtained from calibration to a reference quantity (the calibration factor) is multiplied by the indication value from a measurement, it is possible to obtain the actual measurement value. The calibration was conducted based on an absolute dosimeter from a national calibration center before measurement, which made it possible to establish traceability. In addition, the sensitivity of the ionization chamber is generally proportional to the density of the air inside the ionization volume. If the ionization chamber is exposed to the outside without being sealed, this may influence sensitivity. Because such ionization chambers have different environmental conditions (temperature and pressure) at calibration measurement, the number of air molecules inside the ionization chamber may change. Therefore, it is impossible to obtain precise exposure doses when the calibration factor only is used. We applied Boyle-Charle's law to calculate the calibration coefficient correcting for temperature and pressure in order to calculate the exposure dose. The reference environment conditions for calibration were converted to a temperature of 20°C and a pressure of 1,013 hPa (Eqs 2 and 3) (FDA 2007).

$$\mathrm{K} = \frac{1013}{\mathrm{p}} \times \frac{273.2+\mathrm{t}}{273.2+20} \quad (2)$$

K: calibration coefficient for temperature and pressure, t: temperature when measurement was conducted, p: pressure (hPa)

$$\mathrm{D} = \mathrm{X}_{\mathrm{air}} \times \mathrm{BSF} \times \mathrm{f} \quad (3)$$

D: entrance surface dose (mGy), X_{air}: exposure dose in air depending on distance for each site (R), f: absorbed dose conversion factor (R-Gy conversion factor), BSF: back-scattering factor

2. 2 Evaluation of Image Quality

Acryl phantoms were used to analyze various exposure conditions before the sample image was obtained. In order

to evaluate the quality of the sample image, the DICOM image processing software of Image J (version 1.47k) was used to set the region of interest (ROI). The signal-to-noise ratio (SNR), peak signal-to-noise ratio (PSNR), root mean square error (RMSE), and mean absolute error (MAE) were calculated to compare differences in image quality prior to evaluating the measurement results.

The SNR was used to compare the original image with a restored image (in image compression) to examine the relative quality (in dB). As the dB number increases, the quality of the restored image approaches that of original image (Eq. 4).

$$\mathrm{SNR(dB)} = 10\log_{10}\left(\frac{P_{signal}}{P_{noise}}\right) = 20\log_{10}\left(\frac{A_{signal}}{A_{noise}}\right) \quad (4)$$

PSNR is a measurement of image quality when the original image is set to a standard of 50 dB. In general, when the PSNR is 30 dB or higher, the image quality is excellent, and it is impossible to clinically discern image quality differences (Eq. 5) (Hashimoto *et al*. 2002).

$$\mathrm{PSNR} = 10\log_{10}\left(\frac{\mathrm{MAX}_I^2}{\mathrm{MSE}}\right) = 20\log_{10}\left(\frac{\mathrm{MAX}_I}{\sqrt{\mathrm{MSE}}}\right) \quad (5)$$

For any quantity, the RMSE is calculated at the same location for two sets of data as follows:

$$\mathrm{RMSE} = \sqrt{\frac{1}{N}\sum_{i=1}^{N}(y_i - x_i)^2} \quad (6)$$

Here, x_n, y_n, and N represent the input data column, restored data column, and data column, which are expressed as the average of the squared error.

The signal power is divided by the noise power, but a problem is that there is no signal power that represents all of the images. Since the signal power of a DICOM image is a 12-bit image, $2^{12} = 4096$ was used for calculation.

2. 3 Photon Energy Spectrum

The energy spectrum of an X-ray is dependent on the tube voltage, type of target inside the X-ray tube, anode angle, voltage ripple, and total thickness of the attenuator of the X-ray tube. In our study, the target was tungsten (W), the anode angle was 13 degree, and the voltage was 0because there was no relation with the voltage that was applied to X-ray tube. Inherent filtration was 2.5 mmAl, and an added filter was not used.

An SRS-78 X-ray spectrum simulator was used to conduct simulations of changes in photon fluence depending on changes in kV (Fig. 5).

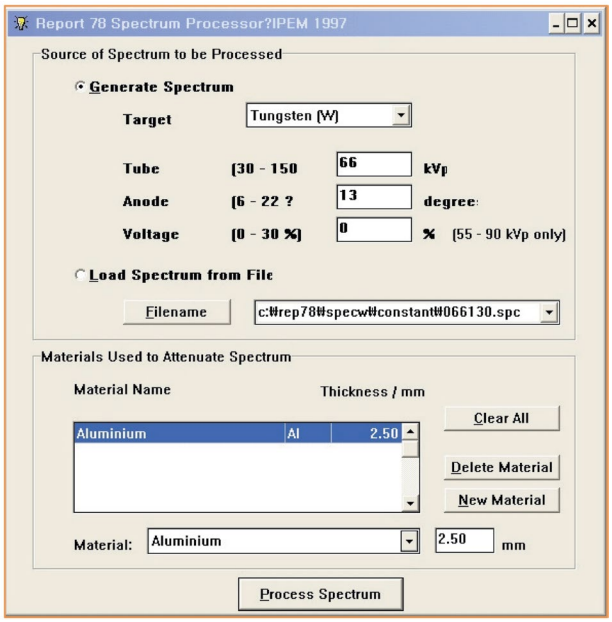

Fig. 5. Photon energy simulation using an SRS-78.

Table 2. Change as a function of mAs and kVp for fixed dose evaluation

No	kVp	mAs	EI[a]	DAP[b] (Gy·cm^2)	ESD[c] (mGy)
1	66	80	32	42.208	3.997
2	66	63	40	19.065	3.152
3	66	50	50	15.129	2.503
4	66	40	63	12.099	1.999
5	66	32	80	9.680	1.596
6	66	25	100	7.561	1.246
7	66	20	125	6.042	0.996
8	66	16	160	4.837	0.794
9	66	12.5	250	3.771	0.611
10	66	10	320	3.018	0.492
11	66	8	400	2.419	0.393
12	66	6.3	500	1.898	0.308
13	66	5	630	1.507	0.245
14	66	4	800	1.204	0.195
15	66	3.2	1000	0.954	0.153
16	66	2.5	1250	0.749	0.119
17	66	2	1600	0.600	0.092

[a]EI is exposure index, [b]DAP is dose area product, [c]ESD is entrance surface dose.

RESULTS

In this study, the ESD value was calculated as the EI, and the DAP and exposure dose were measured for various exposure conditions. Under average exposure conditions of 66 kVp and 12.5 mAs used in our hospitals, the ESD value was

Table 3. Change as a function of kVp and mAs for fixed dose evaluation

No	kVp	mAs	EI[a]	DAP[b] (Gy·cm^2)	ESD[c] (mGy)
1	102	12.5	40	9.216	1.757
2	96	12.5	50	8.180	1.539
3	90	12.5	69	7.183	1.251
4	85	12.5	80	6.414	1.156
5	81	12.5	100	5.803	1.029
6	77	12.5	125	5.222	0.907
7	73	12.5	160	4.688	0.797
8	70	12.5	200	4.267	0.713
9	66	12.5	250	3.771	0.614
10	63	12.5	250	3.402	0.545
11	60	12.5	320	3.035	0.479
12	57	12.5	400	2.697	0.413
13	55	12.5	500	2.474	0.362
14	52	12.5	630	2.139	0.314
15	50	12.5	800	1.917	0.276
16	48	12.5	100	1.719	0.245
17	46	12.5	1250	1.532	0.213

[a]EI is exposure index, [b]DAP is dose area product, [c]ESD is entrance surface dose.

Table 4. ESD (mGy), SNR (dB), PSNR (dB), RMSE, and MAE by changes in mAs

No	mAs	ESD[a] (mGy)	SNR[b] (dB)	PSNR[c] (dB)	RMSE[d]	MAE[e]
1	80	3.997	26.748	28.45	90.836	71.546
2	63	3.152	26.736	28.438	90.959	72.159
3	50	2.503	26.911	28.613	89.143	71.233
4	40	1.999	27.139	28.842	86.83	69.809
5	32	1.596	28.409	30.111	75.024	59.686
6	25	1.246	28.778	30.48	71.903	57.267
7	20	0.996	29.015	30.717	69.969	55.8
8	16	0.794	29.187	30.89	68.592	54.894
9	12.5	0.611	∞	∞	0	0
10	10	0.492	27.509	30.92	84.022	67.144
11	8	0.393	27.011	30.422	88.979	71.232
12	6.3	0.308	26.779	30.19	91.395	73.277
13	5	0.245	26.581	29.992	93.502	75.025
14	4	0.195	26.314	29.725	96.42	77.43
15	3.2	0.153	26.013	29.424	99.82	80.246
16	2.5	0.119	25.592	29.003	104.775	84.396
17	2	0.092	24.969	28.38	112.571	89.575

[a]ESD is entrance surface dose, [b]SNR is signal to noise ratio, [c]PSNR is peak signal to noise ratio, [d]RMSE is root mean square error, [e]MAE is mean absolute error.

0.611. As kVp and mAs increased, the DAP and ESD increased, while EI decreased, and vice-versa (Tables 2 and 3).

Table 5. ESD (mGy), SNR (dB), PSNR (dB), RMSE, and MAE by changes in kVp

No	kVp	ESD[a] (mGy)	SNR[b] (dB)	PSNR[c] (dB)	RMSE[d]	MAE[e]
1	102	1.757	19.372	26.054	203.966	118.709
2	96	1.539	20.475	27.157	179.644	108.726
3	90	1.251	21.831	28.513	153.684	96.572
4	85	1.156	22.887	29.569	136.08	88.947
5	81	1.029	23.899	30.581	121.119	81.426
6	77	0.907	24.596	31.277	111.787	75.439
7	73	0.797	25.691	32.373	98.538	61.782
8	70	0.713	26.067	32.748	94.371	59.569
9	66	0.614	∞	∞	0	0
10	63	0.545	25.446	32.128	101.358	63.694
11	60	0.479	25.023	31.705	106.415	70.378
12	57	0.413	24.925	31.607	107.628	75.037
13	55	0.362	24.456	31.137	113.604	79.726
14	52	0.314	23.735	30.416	123.435	88.952
15	50	0.276	23.245	29.926	130.596	96.717
16	48	0.245	22.595	29.277	140.738	106.043
17	46	0.213	21.777	28.459	154.636	118.877

[a]ESD is entrance surface dose, [b]SNR is signal to noise ratio, [c]PSNR is peak signal to noise ratio, [d]RMSE is root mean square error, [e]MAE is mean absolute error.

Secondly, considering 66 kVp and 12.5 mAs as reference values, SNR (dB), PSNR (dB), RMSE, and MAE values were analyzed to compare image quality as a function of changes in kVp and mAs (Tables 4 and 5).

On the basis of the reference image, SNR (dB) deceased and RMSE and MAE increased. PSNR (dB) was measured at 30 dB or higher from 6.3 mAs to 32 mAs. The equivalent range for kVP was 52 kVp to 81 kVp. Therefore, it was impossible to discern differences in image quality with the naked eye (Fig. 6).

In other words, the ESD without degradation of image quality was 1.596 mGy at 32 mAs and 0.308 mGy at 6.3 mAs (for fixed kVp), a 5.2-fold difference. When mAs were fixed, the ESD was 1.029 mGy at 81 kVp and 0.314 mGy at 52 kVp, a 3.3-fold difference.

Using a reference image at 66 kV, photon energy characteristics and spectrum changes were examined as functions of kV without degradation of image quality. The average value of the photon energy was 43.6 keV at 81 kV, 38.1 keV at 66 kV, and 33 keV at 52 kV. The value of the air kerma, which is the sum of the kinetic energy given to the air, was 169.8 at 81 kV, 119.8 at 66 kV, and 75.27 at 52 kV, a 2.25-fold difference.

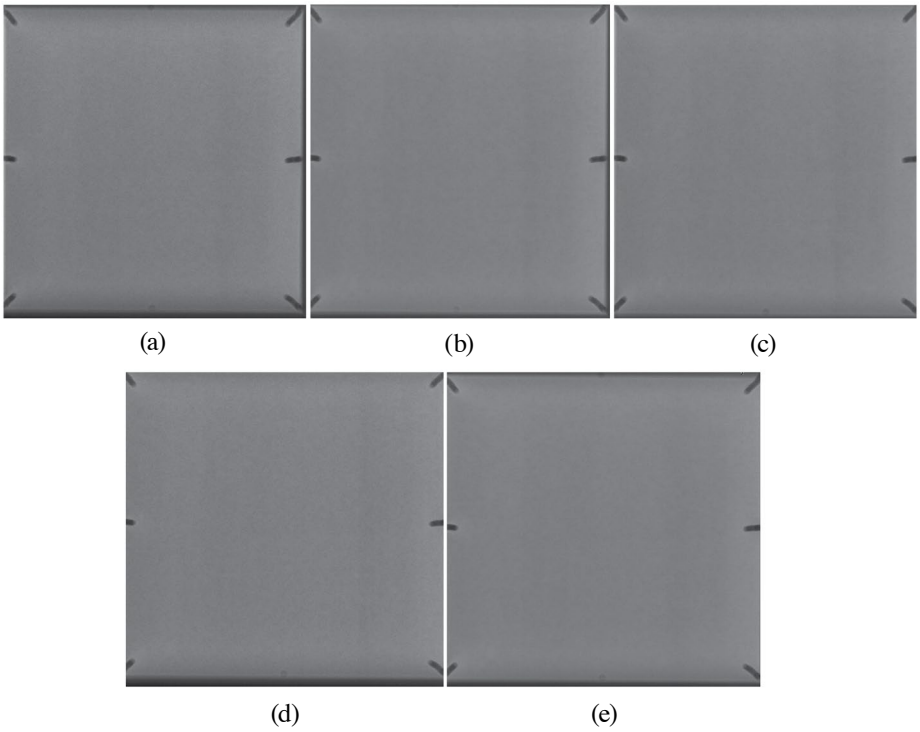

Fig. 6. (a) 52 kVp, 12.5 mAs, (b) 81 kVp, 12.5 mAs, (c) 66 kVp, 12.5 mAs, (d) 66 kVp, 6.3 mAs, and (e) 66 kVp, 32 mAs.

Table 6. Analysis of processed spectra

kV	Mean Photon Energy (keV)	Air Kerma ($\mu Gy \cdot mAs^{-1}$ at 750 mm)	1st HVL[a]
81	43.6	169.8	2.868
77	42.1	155.9	2.710
73	40.6	142.4	2.558
70	39.5	132.5	2.449
66	38.1	119.8	2.311
63	37.1	110.3	2.208
60	36.0	100.8	2.106
57	34.9	91.1	2.005
55	34.1	84.72	1.937
52	33.0	75.27	1.832

[a]HVL is half value layer.

The first HVL was 2.868 mmAl at 81 kV, 2.311 mmAl at 66 kV, and 1.832 mmAl at 52 kV, a 1.56-fold difference in beam quality (Table 6 and Fig. 7).

DISCUSSION

Unlike analog equipment, digital radiation equipment improves image quality thanks to its wide dynamic range and post processing. This enables the reduction of examination repetitions and excessive or deficient doses (Huda *et al*. 1997). The dynamic range can be expressed as the ratio of the maximum to minimum pixel values, which is valid when the absorbed dose of the detector has a linear relationship with pixel value (Rong *et al*. 2001). Film/screen methods have dynamic ranges up to $10^{1.5}$ (1∼30), while digital detectors have ranges up to 10^4 (1∼10000), and so digital detectors have no significant differences in image quality due to changes in dose (compared to film/screen methods) (Hennigs *et al*. 2001). In addition, the brightness of an image from a digital detector can be adjusted in post processing regardless of the exposure dose. Consequently, when the dose is deficient, noise appears in the image, which is likely to be recognized by an examiner. Since unnecessarily excessive doses do not lower image quality, higher doses than necessary are often used.

Since children tend to have low levels of fat inside the head and abdominal cavity as well as small organs, child X-rays often show low image contrast. Examiners must take care to not increase the exposure dose in order to overcome these factors to improve image quality (FDA 2009).

This study found that the exposure dose showed a difference of 5.2 times under examination conditions that did not result in degradation of image quality for various choices of

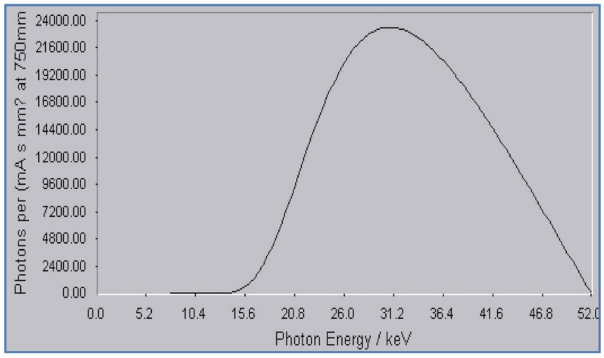

(a)

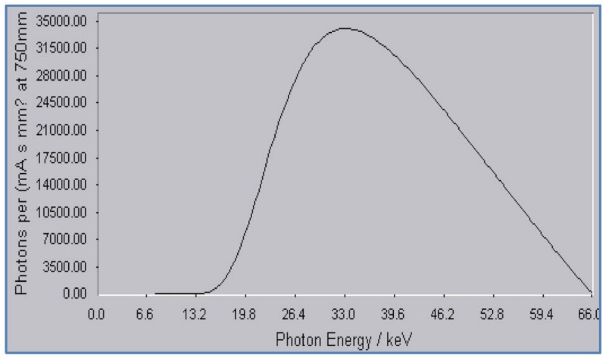

(b)

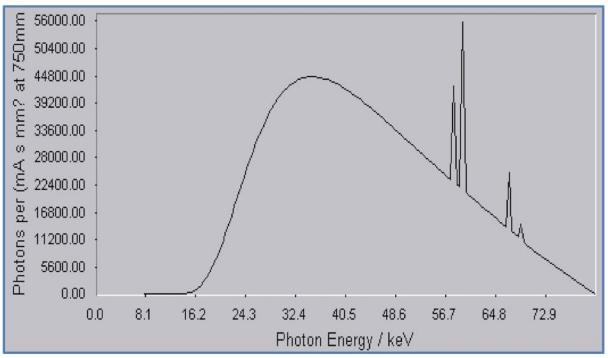

(c)

Fig. 7. Calculated photon spectra at (a) 52 kV, (b) 66 kV, and (c) 81 kV.

kVp and mAs.

In 1996, six international organizations (including the World Health Organization (WHO) and International Atomic Energy Agency (IAEA)) recommended basic safety standards for radiation doses (BSS No. 115). The International Commission on Radiological Protection (ICRP) has required experts in countries around the world to establish international guidelines on the reduction of medical exposure in accordance with the actual conditions of each country. Such diagnostic reference levels (DRL) have various names, including the reference level for patient dose, reference dose level, and guidance level. The concept of a DRL was first introduced by the ICRP. Afterward, the ICRP established the ICRP-73 and supplementary guidelines-2 to recommend the use of the DRL in medical fields (Kim *et al*. 2005). However, even though various organizations have investigated the current state of radiation exposure among adults, there is little data on radiation exposure among children. In South Korea, the Ministry of Food and Drug Safety has established the DRL for each site on the human body. Unfortunately, there have not been any such standards for children less than five years old, except for the chest. Therefore, we believe it is necessary to establish additional standards for radiation exposure on the head, abdomen, and pelvis in order to reduce radiation exposure among children.

Grids, which are used to reduce scattered rays, improve image contrast by reducing the dose in X-ray examinations. However, image quality does not vary much grids are used for examinations of the thin upper limbs or lower limbs. Previous studies have found that it is impossible to discern differences in image quality with the naked eye when the PSNR (dB) is 30 dB or higher, which is consistent with the results found in this study (Kim and Park 2008; Choi *et al*. 2012).

In many medical institutions, it is inconvenient or cumbersome to repeatedly attach and detach grids when they are not necessary (and some equipment does not even allow it), leading to increased exposure. According to a survey by Choi *et al*. of 30 general hospitals in the Seoul metropolitan area, 71.8% of hospitals reported that their equipment that did not enable attachment or detachment of a grid, or that grids were simply not detached due to inconvenience (Choi *et al*. 2012)).

Because many hospitals always use grids, this study was conducted with a grid. Future work should address additional factors that can be adjusted, including the use of a grid, field size, and auto exposure control (AEC) modes for children, and the combination of additional filters for exposure reduction. Examiners should have a clear understanding of the cost-benefit analysis between image quality and increased patient dose before conducting examinations.

CONCLUSIONS

It was confirmed that the difference in exposure dose was

5.2 times at the maximum under the conditions that examination could be conducted without degradation of image quality depending on changes in operating factors of kVp and mAs. Therefore, it is recommended that when examiners need to increase exposure, they should increase kVp, while when they need to decrease exposure, they should decrease mAs. We measured DAP, ESD, and PSNR (dB) under various exposure conditions for head radiographs in children who were highly sensitive to radiation. The image quality was evaluated quantitatively to investigate the necessary levels of radiation exposure. It is believed that the first step toward the reduction in exposure dose is to continue to educate hospitals about the risks of high exposure among children. Furthermore, additional studies on radiation exposure in children should lead to good-quality images with reductions in radiation dose.

ACKNOWLEDGMENTS

The Research has been conducted by the Research Grant of Gwangju Health University in 2020 (2020017).

REFERENCES

Choi SH, Hwang SK, Lee RG, Park YS, Lee JW, Jung HR, Jung JE, Dong KR, Chung WK, Cho JH, Lee J and Ryu YH. 2012. A Study on Evaluating the Image Quality in DR a System with and without a Grid. *J. Korean Phys. Soc.* **60**(11):1977-1982.

Don S. 2004. Radiosensitivity of children: potential for overexposure in CR and DR and magnitude of doses in ordinary radiographic examinations. *Pediatr. Radiol.* **34**:167-172.

FDA. 2007. Patient dose measurement guideline, Radiation Safety Management Series No 14. Food and Drug Administration.

FDA. 2009. Food and Drug Administration, Development of the diagnostic reference level of pediatric chest radiography. Food and Drug Administration. 09142R509.

Hashimoto Y, Seiichi S and Morinaga N. 2002. Channel monitor-based unequal error protection with dynamic OFDM subcarrier assignment for video transmission, IEEE 56th, Vehicular Technology Conference.

Hennigs SP, Garmer M, Jaeger HJ, Classen R, Jacobs A, Gissler HM, Christmann A and Mathias K. 2001. Digital chest radiography with a large-area flat-panel silicon X-ray detector: clinical comparison with conventional radiography. *Eur. Radiol.* **11**(9):688-1696.

Huda W, Nill L and Bruner AP. 1997. Relative speeds of Kodak computed radiography phosphors and screen-film systems. *Med. Phys.* **24**(10):1621-1628.

ICRP. 1990. Recommendations of the International Commission on Radiological Protection. ICRP Publication 60.

ICRP. 2003. International Commission on Radiological Protection, Managing Patient Dose in Digital Radiology. ICRP publication 93.

Jung AY. 2011. Medical radiation exposure in children and dose reduction. J. Korean Med. Assoc. **54**(12):1277-1283.

Kim KH and Park SS. 2012. Measurement of Wi-Fi CCTV Video Service Quality in Wireless Network. *J. Korean Inform. Sci. Soc.* **18**(8):607-611.

Kim WJ, Kim CI, Kim JS, Lee HW and Ryu W. 2008. Research for measuring degradation of IPTV-serviced videos. *J. Broadcast Eng.* **13**(4):440-451.

Kim YH, Choi JH, Oh YH, Lee CH, Cho PK, Kang DH, Lee YB, Kim HC and Kim CM. 2005. Patient exposure doses from medical x-ray examinations in Korea. *J. Radiol. Sci. Technol.* **28**(4):241-248.

Rong XJ, Shaw CC, Liu X, Lemacks MR and Thompson SK. 2001. Comparison of an amorphous silicon/cesium iodide flat-panel digital chest radiography system with screen/film and computed radiography systems-a contrast-detail phantom study. *Med. Phys.* **28**(11):2328-2335.

Shu XO, Potter JD, Linet MS, Severson RK, Han D, Kersey JH, Neglia JP, Trigg ME and Robison LL. 2002. Diagnostic X-rays and ultrasound exposure and risk of childhood acute lymphoblastic leukemia by immunophenotype. *Cancer Epidemiol. Biomarkers Prev.* **11**(2):177-185.

Tanimura M, Matsui I, Abe J, Ikeda H, Kobayashi N, Ohira M, Yokoyama M and Kaneko M. 1998. Increased risk of hepatoblastoma among immature children with a lower birth weight. *Cancer Res.* **58**(14):3032-3035.

UNSCEAR. 2000. United Nations Scientific Committee on the Effects of Atomic Radiation, Source and Effcets of Ionization Radiation. United Nations Scientific Committee on the Effects of Atomic Radiation. Report Vol. I.

Yun OB and Kang HS. 2009. Characteristics of Children Admitted to a Pediatric Emergency Departemnt Following an Accident. *J. Korean Clin. Nurs. Res.* **15**(1):79-91.

Received: 4 July 2020
Revised: 23 July 2020
Revision accepted: 2 September 2020